Coordinated Effects of Sequence Variation on DNA Binding, Chromatin Structure, and Transcription

Helena Kilpinen,[1,2,3]* Sebastian M. Waszak,[2,4]* Andreas R. Gschwind,[2,5]* Sunil K. Raghav,[4] Robert M. Witwicki,[5] Andrea Orioli,[5] Eugenia Migliavacca,[2,5] Michaël Wiederkehr,[5] Maria Gutierrez-Arcelus,[1,2,3] Nikolaos I. Panousis,[1,2,3] Alisa Yurovsky,[1,2,3] Tuuli Lappalainen,[1,2,3] Luciana Romano-Palumbo,[1] Alexandra Planchon,[1] Deborah Bielser,[1] Julien Bryois,[1,2,3] Ismael Padioleau,[1,2,3] Gilles Udin,[4] Sarah Thurnheer,[6] David Hacker,[6] Leighton J. Core,[7] John T. Lis,[7] Nouria Hernandez,[5]† Alexandre Reymond,[5]† Bart Deplancke,[2,4]† Emmanouil T. Dermitzakis[1,2,3,8]†

DNA sequence variation has been associated with quantitative changes in molecular phenotypes such as gene expression, but its impact on chromatin states is poorly characterized. To understand the interplay between chromatin and genetic control of gene regulation, we quantified allelic variability in transcription factor binding, histone modifications, and gene expression within humans. We found abundant allelic specificity in chromatin and extensive local, short-range, and long-range allelic coordination among the studied molecular phenotypes. We observed genetic influence on most of these phenotypes, with histone modifications exhibiting strong context-dependent behavior. Our results implicate transcription factors as primary mediators of sequence-specific regulation of gene expression programs, with histone modifications frequently reflecting the primary regulatory event.

Functional genomic elements have been linked to specific chromatin signatures in different cell types (*1*), illustrating control of transcriptional processes through multiple layers of genome organization. Although allele-specific gene expression is widespread (*2*), it has been difficult to pinpoint the upstream cis-regulatory variants and how they affect chromatin states. We performed chromatin immunoprecipitation (ChIP) of five histone posttranslational modifications (hPTMs) (H3K4me1, H3K4me3, H3K27ac, H3K27me3, and H4K20me1), three transcription factors (TFs) (TFIIB, PU.1, and MYC), and the second largest RNA polymerase II subunit RPB2 (POLR2B) (fig. S1) in lymphoblastoid cell lines (LCLs) derived from two parent-offspring trios (*3*). A subset of the ChIP assays was also performed in eight additional unrelated individuals. We further profiled one of the trios with global run-on sequencing (GRO-seq), which measures nascent transcription at all transcribed regions (fig. S2), and examined available deoxyribonuclease I (DNase I)–seq and CCCTC-binding factor (CTCF) ChIP-seq data (*4*). All 14 individuals were additionally profiled for mRNA expression (*5*). Clustering of the molecular phenotypes along promoters and enhancers was consistent with published reports (*1*) (figs. S3 to S5).

We identified sites of allele-specific (AS) TF binding, hPTM, and transcription for all assays (*5*), ranging from 11 to 12% for TFs (*4*, *6*) to 6 to 30% for hPTMs at heterozygous sites accessible for the analysis (median across all individuals) (Fig. 1A and fig. S6). Notably, in the two trios, fewer AS effects were observed in mRNA (mRNA-seq, 5%) than in nascent transcripts (GRO-seq, 27 to 28%) (*5*), likely reflecting posttranscriptional modifications.

Multiple heterozygous single-nucleotide polymorphisms (SNPs) overlapping regions of TF activity showed high consistency in allelic direction within individuals (Fig. 1B and fig. S7, A and B). Allelic consistency in nascent transcripts and histone modifications was high even with sites several kilobases apart and decreased with genomic distance (logistic regression, $P < 0.05$; fig. S7C). The strongest AS effects were enriched at promoters, whereas the allelic signals of marks of enhancer activity (PU.1, H3K4me1, H3K27ac) or heterochromatin (H3K27me3) showed a more dispersed distribution (fig. S8). We also analyzed all accessible heterozygous SNPs overlapping known expression quantitative trait loci (eQTLs) from the 1000 Genomes phase 1 populations (*5*, *7*) and observed an enrichment of allelic bias at eQTLs relative to non-eQTLs for TFs ($P = 0.016$, Mann-Whitney *U* test) but not for hPTMs (fig. S9); this finding suggests that a TF binding change is often causal to the gene expression change.

Linking hPTM signatures with specific DNA sequence features has proven difficult (*8*), but for sequence-specific TFs it is possible to assess whether the observed AS effects are due to motif-disrupting variants (fig. S10). Categorization of significant AS binding sites, with respect to predicted TF motifs, revealed three classes of binding SNPs (B-SNPs): B-SNPs located either within (class I) or adjacent to (class II) predicted PU.1 and MYC consensus TF motifs, or B-SNPs in motif-devoid peaks (class III). Class I sites were enriched for B-SNPs relative to the other two classes (fig. S11, A and B, for PU.1; fig. S12, A and B, for MYC), which suggests that SNP-mediated disruption of the TF motif is likely causal to the observed AS binding activity. However, most TF AS binding events (70%, PU.1; 97%, MYC) appear triggered through TF consensus motif–independent mechanisms (figs. S11A and S12A) (*6*, *9*). For example, allelic binding cooperativity tests (*5*) revealed four additional motifs

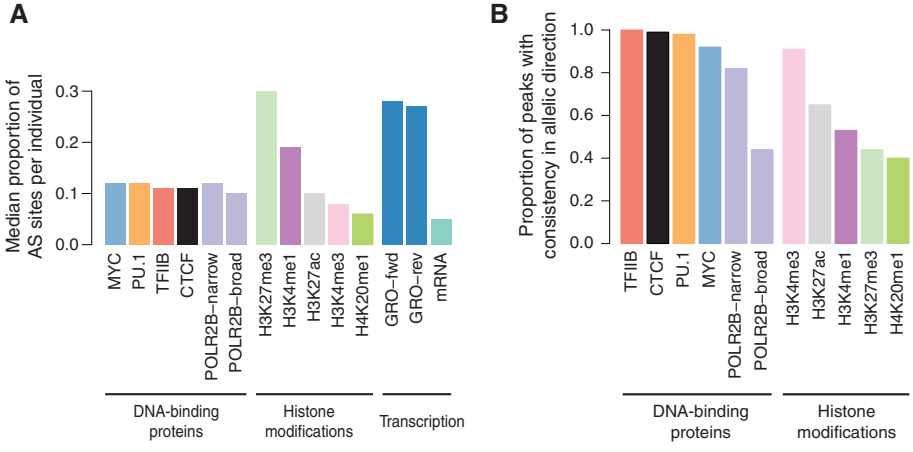

Fig. 1. Allele-specific (AS) activity within transcriptional and chromatin layers. (**A**) Proportion of accessible heterozygous SNP sites showing significant AS activity (median across all individuals, $n = 3$ to 14). (**B**) Consistency of allelic effects within genomic regions of TF binding and histone modification. Bars represent the proportion of peaks with a consistent allelic direction at two or more SNP sites.

[1]Department of Genetic Medicine and Development, University of Geneva Medical School, 1211 Geneva, Switzerland. [2]Swiss Institute of Bioinformatics, 1015 Lausanne, Switzerland. [3]Institute of Genetics and Genomics of Geneva, University of Geneva, 1211 Geneva, Switzerland. [4]Laboratory of Systems Biology and Genetics, Institute of Bioengineering, School of Life Sciences, Swiss Federal Institute of Technology (EPFL), 1015 Lausanne, Switzerland. [5]Center for Integrative Genomics, Faculty of Biology and Medicine, University of Lausanne, 1011 Lausanne, Switzerland. [6]Protein Expression Core Facility, School of Life Sciences, Swiss Federal Institute of Technology (EPFL), 1015 Lausanne, Switzerland. [7]Department of Molecular Biology and Genetics, Cornell University, Ithaca, NY 14850, USA. [8]Center of Excellence in Genomic Medicine Research, King Abdulaziz University, Jeddah 21589, Saudi Arabia.

*These authors contributed equally to this work.
†Corresponding author. E-mail: emmanouil.dermitzakis@unige.ch (E.T.D.); bart.deplancke@epfl.ch (B.D.); alexandre.reymond@unil.ch (A.R.); nouria.hernandez@unil.ch (N.H.)

(NFKB1, POU2F2, PRDM1, and STAT2), located proximal to the PU.1-bound site, that show covariance with AS PU.1 binding activity [false discovery rate (FDR) = 5%; Fig. 2A and fig. S13] and collectively explain another 7.5% of AS PU.1 binding activity.

Despite a strong correlation between motif score differences and AS binding (figs. S11C and S12C; >90% expected direction), we observed that the majority of motif-disrupting SNPs do not show significant allelic effects (figs. S11A and S12A). Therefore, we tested whether homotypic TF motifs (i.e., multiple motifs for the same TF) located within PU.1-bound regions might buffer the effects of motif-disrupting SNPs (*5*, *10*, *11*) and found that TF-bound regions with homotypic motifs exhibit fewer allelic effects (41% versus 25%; $P = 0.0087$, Mann-Whitney U test). In addition, the impact of SNPs on TF motifs scales with the likelihood of observing significant AS effects (Fig. 2B and fig. S12D), but this trend is not significant if a second, unaffected homotypic TF motif is located nearby (Fig. 2B and fig. S11D). These results suggest that homotypic motif clusters buffer the effect of genetic variation over several similar binding sites.

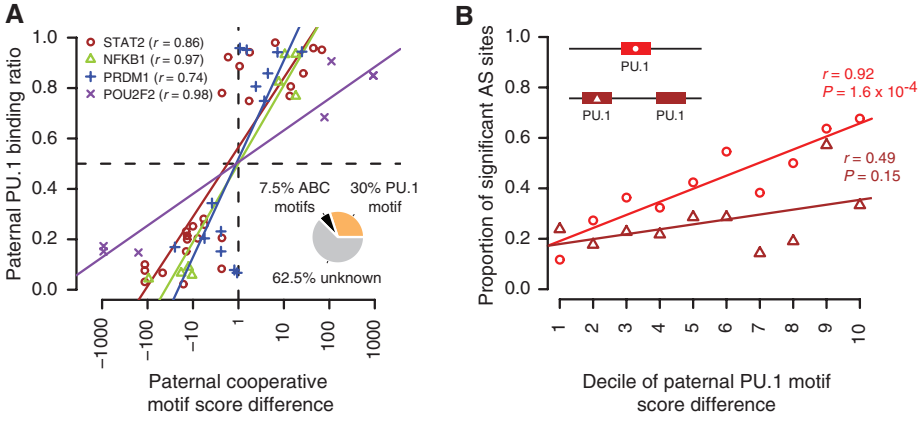

Fig. 2. DNA sequence properties at allele-specific PU.1 binding sites. (**A**) SNPs in PU.1-bound and cooperative TF motifs are predictive of AS PU.1 binding (5% FDR) (*5*). (**B**) PU.1-bound regions (peaks) with homotypic PU.1 motifs show a weak response toward motif-disrupting SNPs. Motif-disrupting SNPs were split into two classes (one or two PU.1 motifs per peak) and grouped according to their motif impact (1, lowest; 10 highest).

We investigated the genetic component of allele-specific chromatin and binding signals by (i) comparing the direction of allelic bias at shared significant AS sites across 10 unrelated individuals (Fig. 3A), and (ii) testing for transmission of allelic effects from parents to children (Fig. 3B and fig. S17) (*4*). Allelic directions at shared significant AS sites in the unrelated individuals were significantly correlated ($P < 0.05$, Spearman correlation; fig. S16A), with mRNA showing the highest degree of consistency in allelic directions between individuals, followed by TF binding and histone modification, respectively (Fig. 3A and figs. S14 to S16). We observed evidence of

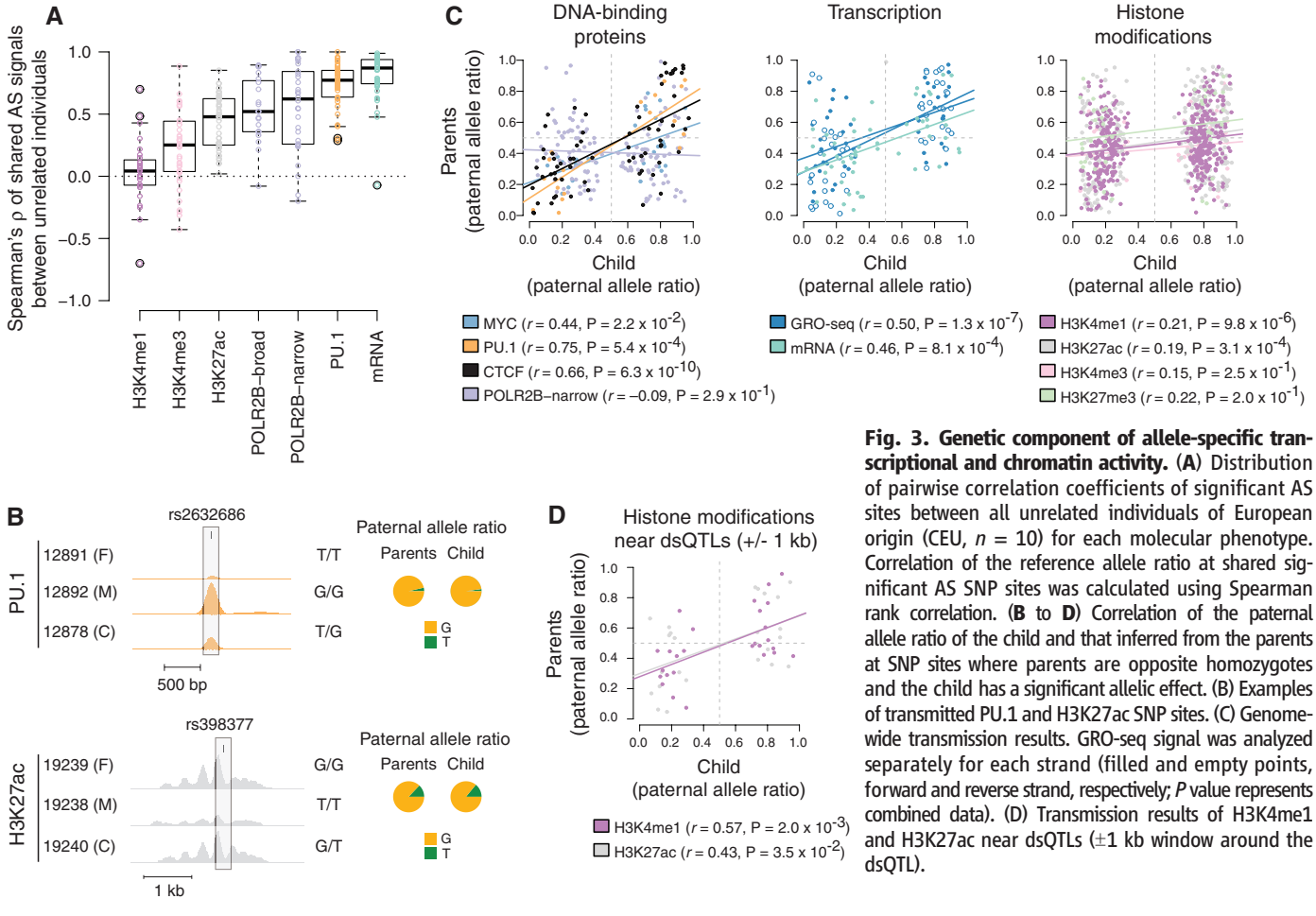

Fig. 3. Genetic component of allele-specific transcriptional and chromatin activity. (**A**) Distribution of pairwise correlation coefficients of significant AS sites between all unrelated individuals of European origin (CEU, $n = 10$) for each molecular phenotype. Correlation of the reference allele ratio at shared significant AS SNP sites was calculated using Spearman rank correlation. (**B** to **D**) Correlation of the paternal allele ratio of the child and that inferred from the parents at SNP sites where parents are opposite homozygotes and the child has a significant allelic effect. (B) Examples of transmitted PU.1 and H3K27ac SNP sites. (C) Genome-wide transmission results. GRO-seq signal was analyzed separately for each strand (filled and empty points, forward and reverse strand, respectively; *P* value represents combined data). (D) Transmission results of H3K4me1 and H3K27ac near dsQTLs (±1 kb window around the dsQTL).

significant parental transmission with all three regulatory TFs (ρ = 0.44 to 0.75, $P \leq 0.02$, Spearman correlation; Fig. 3C and fig. S17), consistent with their strong sequence dependence (*4*, *6*). For hPTMs, evidence of transmission was detected for the active histone marks H3K4me1, H3K4me3, and H3K27ac (ρ = 0.12 to 0.21; $P \leq 0.02$), but their level of transmission was lower than for TFs. Transmission signals for mRNA levels and nascent transcription were significant and comparable to TFs (ρ = 0.46 and 0.50; $P = 0.0008$ and $P = 1.3 \times 10^{-7}$, respectively). We observed only weak transmission for POLR2B (fig. S17), possibly due to the distinct activity states of the polymerase (*12*). We determined the genetic control of the transmission signal of histone marks at known eQTLs (*7*) and DNase I sensitivity QTLs (dsQTLs) (*13*), respectively, because the former are enriched within TF binding sites (*13*). Transmission of the active marks H3K4me1, H3K4me3, and H3K27ac was stronger near eQTLs and dsQTLs (ρ = 0.31 to 0.57) than genome-wide (Fig. 3D and fig. S20), which suggests that the transmission behavior of the overall chromatin state depends on the properties of the underlying sequence. Collectively, these findings indicate coordinated and genetically driven changes between TF binding and histone modifications, and suggest that TFs are the primary determinants of regulatory interactions (*14*–*16*).

To further assess the extent of allelic coordination (AC) between distinct genomic regulatory layers, we calculated the correlation between AS effects across pairs of molecular phenotypes (fig. S21). We observed that each testable phenotype exhibits significant correlation in allelic ratios with one or multiple phenotypes (Spearman correlation, $P < 0.05$). The majority of AC events reflect relationships between distinct regulatory layers that have also been observed quantitatively [e.g., POLR2B-H3K4me3 at promoters (*1*, *17*, *18*); GRO-seq–H3K4me1–H3K27ac at putative enhancers (*19*)] (Fig. 4A and fig. S21). These results support a strong allelic (i.e., local) interconnectivity among regulatory and general TFs, histone modifications, and transcription.

eQTLs are often located distal to their target genes (*20*), indicating that allelic signals within regulatory layers might extend over short and long distances. We examined haplotypic coordination (HC)—defined as long-range coordination in allelic direction on the same chromosome—of AS effects at nonoverlapping heterozygous sites (*5*) (Fig. 4B and fig. S21), and found that every TF and histone mark exhibits HC with one or more regulatory layer(s) around genes and their flanking regions (fig. S21; Spearman correlation, $P < 0.05$). The degree of coordination varied between regulatory layers, ranging from −0.24 (GRO-seq–CTCF; $P = 0.03$) to 0.64 (MYC-mRNA; $P = 2.9 \times 10^{-8}$). The majority (>90%) of significant HC events were positive; that is, the allelic bias co-occurred on the same haplotype (Fig. 4B and fig. S21). For 25% of assay pairs tested, the strength of HC was significantly correlated with the genomic distance between SNP pairs (logistic regression, $P < 0.05$; odds ratio = 0.19 to 2.2) (fig. S22). For example, the enhancer-associated histone marks H3K4me1 and H3K27ac showed allelic consistency up to 200 kb with the TF PU.1. Thus, a single or few variant(s) likely trigger long-distance allelic effects over many of the regulatory layers acting on a genomic region.

Our work has revealed abundant allele-specific activity across all regulatory layers. Parental transmission of the allelic effects suggests that DNA sequence variations affecting transcription, TF binding, and histone modifications are largely transmitted from parents to children, with allelic histone effects showing more context-dependent behavior compared to TFs. Coordinated allelic and haplotypic behavior at different functional elements of the genome suggest that TF binding, histone modifications, and transcription operate within the same allelic framework. This is consistent with the fact that a few TFs can induce cellular reprogramming and massive changes in the chromatin landscape (*21*), and that the maintenance of a transcription-permissive environment and transcriptional memory are independent of histone modifications (*22*). Both histone modifications and TF binding are under genetic control, but histone modifications are more prone to stochastic, possibly transient effects and likely reflect (*23*), rather than define, coordinated regulatory interactions.

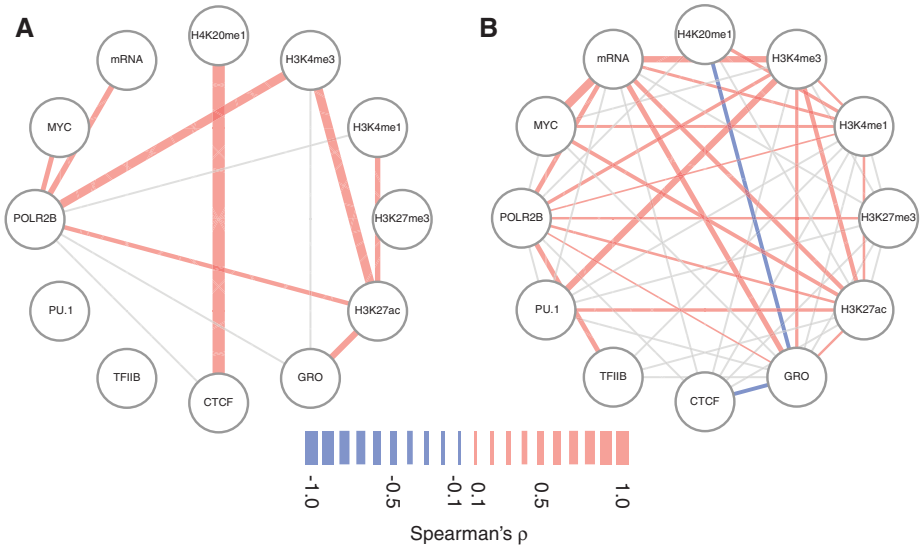

Fig. 4. Local, short- and long-range coordination between transcriptional and chromatin layers. Results of allelic coordination (**A**) and haplotypic coordination (**B**) analysis at gene regions (genes ± 50 kb) (*5*). Coordination of the allelic effect was considered between all pairs of assays. SNP sites within genomic regions were required to show a significant AS effect in both assays. Only assay pairs with ≥20 SNPs were considered for the analysis. Significant Spearman rank correlation coefficients ($P < 0.05$) between the paternal allele ratios of the SNP pairs are indicated with colored lines ranging in intensity from ρ = −1.0 (blue) to ρ = 1.0 (red). Nonsignificant correlations are indicated with gray lines; missing lines indicate lack of sufficient data points for analysis.

References and Notes

1. B. E. Bernstein *et al.*, *Nature* **489**, 57–74 (2012).
2. S. B. Montgomery *et al.*, *Nature* **464**, 773–777 (2010).
3. G. R. Abecasis *et al.*, *Nature* **467**, 1061–1073 (2010).
4. R. McDaniell *et al.*, *Science* **328**, 235–239 (2010).
5. See supplementary materials on *Science* Online.
6. T. E. Reddy *et al.*, *Genome Res.* **22**, 860–869 (2012).
7. T. Lappalainen *et al.*, *Nature* **501**, 506–511 (2013).
8. S. Henikoff, A. Shilatifard, *Trends Genet.* **27**, 389–396 (2011).
9. M. Kasowski *et al.*, *Science* **328**, 232–235 (2010).
10. M. T. Maurano, H. Wang, T. Kutyavin, J. A. Stamatoyannopoulos, *PLOS Genet.* **8**, e1002599 (2012).
11. M. Spivakov *et al.*, *Genome Biol.* **13**, R49 (2012).
12. L. J. Core, J. J. Waterfall, J. T. Lis, *Science* **322**, 1845–1848 (2008).
13. J. F. Degner *et al.*, *Nature* **482**, 390–394 (2012).
14. D. H. Erwin, E. H. Davidson, *Nat. Rev. Genet.* **10**, 141–148 (2009).
15. O. Hobert, *Curr. Biol.* **21**, R146–R147 (2011).
16. M. Ptashne, *Curr. Biol.* **17**, R233–R236 (2007).
17. C. Y. Lin *et al.*, *Cell* **151**, 56–67 (2012).
18. Z. Nie *et al.*, *Cell* **151**, 68–79 (2012).
19. D. Wang *et al.*, *Nature* **474**, 390–394 (2011).
20. E. Grundberg *et al.*, *Nat. Genet.* **44**, 1084–1089 (2012).
21. C. A. Doege *et al.*, *Nature* **488**, 652–655 (2012).
22. R. Margueron, D. Reinberg, *Nat. Rev. Genet.* **11**, 285–296 (2010).
23. M. Gutierrez-Arcelus *et al.*, *Elife* **2**, e00523 (2013).

Acknowledgments: Supported by Swiss National Science Foundation grants CRSI33_130326 (E.T.D., B.D., A.R., N.H.), 31003A_132958 (N.H.), 31003A_130342 (E.T.D.), and 31003A_129835 (A.R.); the European Research Council (E.T.D.); the Louis-Jeantet Foundation (E.T.D.); European Molecular Biology Organization fellowship ALTF 2010-337 (H.K.); a fellowship from the doctoral school of the Faculty of Biology and Medicine, University of Lausanne (R.M.W.); the NCCR Frontiers in Genetics Program (M.G.-A., J.B., E.T.D., B.D.); the Japanese-Swiss Science and Technology Cooperation

Program (Japan Science and Technology Agency/ETH Zürich) (B.D.); École Polytechnique Fédérale de Lausanne (B.D.); and NIH grants HG004845 and GM25232 (J.T.L.). The computations were performed at the Vital-IT (www.vital-it.ch) Center for High-Performance Computing of the Swiss Institute of Bioinformatics. All data in this publication are available through ArrayExpress (www.ebi.ac.uk/arrayexpress/) under accession numbers E-MTAB-1883 (RNA-seq), E-MTAB-1884 (CHiP-seq), and E-MTAB-1885 (GRO-seq). The authors declare no competing financial interests.

Supplementary Materials
www.sciencemag.org/content/342/6159/744/suppl/DC1
Materials and Methods
Figs. S1 to S31
Tables S1 and S2
References (*24*–*39*)

26 June 2013; accepted 12 September 2013
Published online 16 October 2013;
10.1126/science.1242463

Identification of Genetic Variants That Affect Histone Modifications in Human Cells

Graham McVicker,[1,2]* Bryce van de Geijn,[1,3]* Jacob F. Degner,[1,3] Carolyn E. Cain,[1] Nicholas E. Banovich,[1] Anil Raj,[1,4] Noah Lewellen,[2] Marsha Myrthil,[2] Yoav Gilad,[1]† Jonathan K. Pritchard[1,2,4,5]†

Histone modifications are important markers of function and chromatin state, yet the DNA sequence elements that direct them to specific genomic locations are poorly understood. Here, we identify hundreds of quantitative trait loci, genome-wide, that affect histone modification or RNA polymerase II (Pol II) occupancy in Yoruba lymphoblastoid cell lines (LCLs). In many cases, the same variant is associated with quantitative changes in multiple histone marks and Pol II, as well as in deoxyribonuclease I sensitivity and nucleosome positioning. Transcription factor binding site polymorphisms are correlated overall with differences in local histone modification, and we identify specific transcription factors whose binding leads to histone modification in LCLs. Furthermore, variants that affect chromatin at distal regulatory sites frequently also direct changes in chromatin and gene expression at associated promoters.

Variation at noncoding regulatory sequences contributes to the genetics of complex traits (*1*–*3*), yet we still have limited understanding of the primary mechanisms by which they act. One possibility is that regulatory variants affect histone modifications that have downstream consequences on chromatin remodeling or transcription (*4*). There are many possible posttranslational modifications of histones (i.e., "histone marks") (*4*), and sets of these co-occur in distinct chromatin states (*5*–*9*), are associated with functional elements (*2*, *10*, *11*), and are sensitive indicators of changes in gene regulation (*9*, *12*). However, we still do not know whether histone modifications are generally a cause or a consequence of gene regulation or which DNA elements direct cell type–appropriate histone marking (*7*, *13*). Thus, studies of genetic variants that disrupt transcription factor binding sites (TFBSs) may illuminate whether histone modifications enable transcription factor binding or whether the binding of transcription factors results in histone modification.

We performed chromatin immunoprecipitation followed by sequencing (ChIP-seq) for RNA polymerase II (Pol II) and four posttranslational modifications of histone H3 (H3K4me1, H3K4me3, H3K27ac, and H3K27me3) in 10 unrelated Yoruba lymphoblastoid cell lines (LCLs). H3K4me3 (trimethylation of lysine 4) is primarily associated with active promoters; H3K4me1 (monomethylation of lysine 4) is associated with active chromatin outside of promoters (e.g., enhancers); H3K27ac (acetylation of lysine 27) is associated with both active promoters and enhancers (*6*, *14*); and H3K27me3 (trimethylation of lysine 27) is associated with silencing by the polycomb repressive complex 2 (PRC2) (*15*, *16*). We mapped the ChIP-seq reads to the human genome, controlling for mapping biases introduced by polymorphic sites (*17*). Comparisons with ENCODE (*1*) showed consistent distributions of each mark (fig. S1).

To identify genetic associations with histone marks and Pol II, we developed a "combined haplotype test" that uses both read depth and allelic imbalance to enable mapping of cis–quantitative trait loci (QTLs) with small sample sizes (*17*). We applied the combined haplotype test to hundreds of thousands of polymorphic sites with sufficient read depth (i.e., sites within ChIP-seq peaks) and identified more than 1200 histone mark and Pol II QTLs at a false discovery rate (FDR) of 20% (Fig. 1, A and B, and fig. S3). After merging overlapping regions, we identified a total of 27 distinct QTLs for H3K4me1, 469 for H3K4me3, 730 for H3K27ac, 118 for Pol II, and 2 for H3K27me3 (which tends not to fall into strong peaks) (table S2). At an FDR threshold of 10%, we identified 582 distinct histone mark and Pol II QTLs (table S2). In principle, some of these signals might be due to imprinting (*8*) or random allelic inactivation; however, several lines of evidence indicate that most of the regions that we identify are conventional QTLs (supplementary text).

Many of the histone mark QTLs overlap previously identified QTLs for deoxyribonuclease (DNase I) sensitivity (denoted "dsQTLs") (*18*). DNase I sensitivity is an indicator of open chromatin, and DNase I hypersensitive sites (DHSs) typically mark active regulatory regions that are associated with active histone marks and transcription factor binding (*19*). Indeed, we found an enrichment of low *P* values when testing for QTL associations with Pol II and all four histone marks at dsQTLs, compared to the genome-wide set of tested single-nucleotide polymorphisms (SNPs) (Fig. 1, A and B, and fig. S3). Nevertheless, although most histone mark and Pol II QTLs are within 1 kb of a DHS (table S5), many are far from known dsQTLs (fig. S8). This suggests that histone modifications may provide more power to detect differences in chromatin state beyond that of DNase I sensitivity.

We plotted aggregate ChIP-seq read depth around DHSs associated with dsQTLs (Fig. 2), grouping read counts according to whether an individual carries the genotype associated with high, medium, or low sensitivity at a dsQTL. Most of the dsQTLs lie outside promoters, and the average histone mark read depths at dsQTL DHSs follow qualitative expectations for distal enhancers (*6*), with higher levels of H3K4me1 and lower levels of H3K4me3 and Pol II as compared to promoters. High-sensitivity genotypes tend to have reduced nucleosome occupancy within the DHS (*20*); higher levels of transcription factor binding (*18*); higher levels of the active marks H3K4me1, H3K4me3, and H3K27ac; and higher Pol II occupancy. The relation between DNase I and the repressive mark H3K27me3 is more complicated, as we find both positive and negative associations. We find no opposite-direction effects between DNase I and either H3K4me1, H3K4me3, or H3K27ac (fig. S5).

At expression QTLs (eQTLs) (*21*), we stratified the samples by the genotype of the most significant eQTL SNP and found overall patterns similar to those at dsQTLs (Fig. 2). Individuals who are homozygous for the high-expression genotype generally have higher levels of DNase I sensitivity, H3K4me3, H3K27ac, and Pol II

[1]Department of Human Genetics, University of Chicago, Chicago, IL 60637, USA. [2]Howard Hughes Medical Institute, Stanford University, Stanford, CA 94305, USA. [3]Committee on Genetics, Genomics and Systems Biology, University of Chicago, Chicago, IL 60637, USA. [4]Department of Genetics, Stanford University, Stanford, CA 94305, USA. [5]Department of Biology, Stanford University, Stanford, CA 94305, USA.

*These authors contributed equally to this work.
†Corresponding author. E-mail: gilad@uchicago.edu (Y.G.); pritch@stanford.edu (J.K.P.)

Coordinated Effects of Sequence Variation on DNA Binding, Chromatin Structure, and Transcription

Helena Kilpinen *et al.*

Science **342**, 744 (2013);
DOI: 10.1126/science.1242463

Science (print ISSN 0036-8075; online ISSN 1095-9203) is published weekly, except the last week in December, by the American Association for the Advancement of Science, 1200 New York Avenue NW, Washington, DC 20005.